Photodiagnosis and Photodynamic Therapy 29 (2020) 101577

Contents lists available at ScienceDirect

Photodiagnosis and Photodynamic Therapy

journal homepage: www.elsevier.com/locate/pdpdt

A New handheld singlet oxygen detection system (SODS) and NIR light source based phantom environment for photodynamic therapy applications

Ali Furkan Kamanli[a,*], Gökçen Çetinel[b], Mustafa Zahid Yıldız[a]

[a] Sakarya University of Applied Sciences, Faculty of Technology, Electrical and Electronics Engineering, Turkey
[b] Sakarya University, Faculty of Engineering, Electrical and Electronics Engineering, Turkey

A B S T R A C T

Photodynamic therapy (PDT) is an emerging treatment modality in various areas such as cancer treatment and disinfection. The photosensitizer and oxygen have crucial roles for effective PDT treatment. The quantitative evaluation of singlet oxygen, which is a gold standard for monitoring effective treatment, remains as an important problem for PDT. However, low quantum yield and low life span of the singlet oxygen make the system expensive, unnecessarily large and unadaptable for clinical usage. In our study, a new mobile singlet oxygen detection system (SODS) was designed to detect singlet oxygen illumination during PDT and a new singlet oxygen phantom environment was constituted to test the designed SODS system.

The singlet oxygen phantom environment composed of fast switching led driver & microcontroller and led light source (1200 − 1300 nm radiation). The elements of the singlet oxygen detection system are optic filter and collimation, avalanche photodiode transimpedance amplifier, differential amplifier and a signal processing block. According to the performance evaluation of the system on the phantom environment, the presented SODS can measure the illuminations at 1270 nm wavelength between 10 ns and 15 μs timespans. The results showed that the proposed system might be a good candidate for clinical PDT applications.

1. Introduction

Photodynamic therapy (PDT) is defined as a photochemotherapy method based on the principle of irradiating the target lesion with an appropriate wavelength of the light sources by local or systemic agents [1,2]. This method is being used for the treatment of cancer, infection and rheumatoid arthritis. After PDT, the body recovers itself more easily.

PDT involves the combination of photosensitive substance, low-energy visible light and an oxygen molecule to destroy the undesired target [3–6]. Each of the components constituting this combination is not therapeutic alone. The necessary treatment elements of the therapy are the presence of molecular oxygen in the tissue, photosensitizing agent and the special light source [7]. If the wavelength of light source matches the peak level in the absorption spectrum of a photosensitizer (PS), the resulting reaction will be even more effective. Following the light absorption, the PS is stimulated to a higher energy state [8–10].

Singlet oxygen, which is a major component of many biological processes and acts as a cytotoxic agent in cancer treatment with PDT, is the triplet state of the molecular oxygen [11,12]. Singlet oxygen is produced by a photosensitive process comprising a light source of a particular wavelength, a photosensitizer, and molecular oxygen [13,14]. The physical vital factors such as blood flow, local tissue oxygenation, photo-bleaching, and dosimetry factors of photosensitizers have a significant role on PDT efficiency [15,16].

Monitoring the singlet oxygen molecule formed during PDT gives information about whether the treatment is successful or not. Thereby, singlet oxygen measurement is very important in the treatment process [3–7,17,18]. The amount and location of this molecule must be taken into account to evaluate the performance of therapy [19–21]. Implicit dosimetry, open dosimetry, and biophysical/biological tissue response monitoring techniques have been developed for effective PDT [22–24]. Singlet Oxygen Luminescence Dosimetry (SOLD), is a promising singlet oxygen 1270 nm illumination detection method which is accepted as a prominent technique for PDT applications [17,25–27]. Moreover, this specific luminescence has a very short lifetime and low-level quantum yield when it interacts with the biological environment during the actual treatment [28,29].

In recent years, singlet oxygen detection systems have been developed in order to build closed-loop PDT treatment modalities, which are large monochromatic-based instruments including IR PMTs (Infrared Photomultiplier Tube) and InGaAs SPADs (Indium Gallium Arsenic Single Photon Avalanche Detectors) [30–34]. These systems cannot be easily applied to clinical usage without further research. On the other hand, the difficulties on the measurement of the singlet oxygen life span and the oxygenation rate of the tissue make the system cost higher and hard to implement in clinical treatment. Considering these difficulties, the sensitivity of the system should be determined in a phantom

* Corresponding author.
E-mail address: fkamanli@sakarya.edu.tr (A.F. Kamanli).

https://doi.org/10.1016/j.pdpdt.2019.10.012
Received 22 July 2019; Received in revised form 2 October 2019; Accepted 11 October 2019
Available online 08 November 2019
1572-1000/

environment. During PDT, multi-parameter simultaneous detection is required. Various single-parameter detection methods have been used to investigate and evaluate the treatment process. These methods confirm that the amount of singlet oxygen is strongly correlated with cell life. However, there is no valid quantitative relationship between them. Therefore, the success and traceability of PDT can be ensured by actively monitoring the singlet oxygen molecule.

In this study, a new Singlet Oxygen Detection System (SODS) and a new singlet oxygen luminescence based tissue phantom environment was designed. The proposed system is cost-effective, mobile, specially designed for Singlet oxygen and has the ability to interact low level and short life-cycle illumination. The captured luminescence interval with this system was between 10 ns-15 μs at 1270 nm wavelength. In future studies, our goal is to combine SODS to a closed-loop PDT system which can be used for cancer treatment. The combination of SODS and light dosimetry leads to more successful treatments. The phantom environment developed for more accurate limitation measurement and for implementation of SOED or SOLD based mimicking the clinical and laboratory experiment without any chemicals and experimental procedures.

The study was organized as follows. In Section 2, the proposed system was introduced. Each component of the system was discussed to better understand the study. In Section 3, the experimental results to evaluate the performance of the proposed system was given. The accuracy of the experimental results was validated by means of mathematical calculations, in Section 4. Finally, Section 5 concluded the paper.

2. Material and method

In this section, the fast switching light source, which was evaluated as a phantom environment, and the singlet oxygen detection system were introduced. The fast switching light source consisted of two components: fast switching led driver & microcontroller and led light source (1200 − 1300 nm). The elements of the singlet oxygen detection system were optic filter and collimation, avalanche photodiode transimpedance amplifier, differential amplifier and signal processing blocks as indicated in Fig. 1. The details of the proposed system were given below.

2.1. Fast switching light source based phantom environment

Phantom singlet oxygen luminescence environment was controlled with an Arm-based microcontroller having a high-speed switching capability, to radiate around the 1200-1300 nm and containing a tissue intra-lipid for precise mimicking the environment that forming the singlet oxygen illumination. The system was controlled around 0 to the 216 MHz frequency and on fW-mW optic power level which could give a perfect imitation of singlet oxygen luminescence. Optic power was calibrated with Thorlabs brand femtowatt-level light detection module.

On the fast switching light source, LEDs were connected to PD12-PD13 pins of the timer 4 as shown in Fig. 2a. The LEDs are Thorlabs brand 1200 L and 1300E product which have a 5 mW power at 1200 nm and 2 mW power at 1200 nm for 10 cm distance, respectively. LEDs were chosen according to their imitation to un-even light distribution which can be compared to singlet oxygen illumination on PS solution. The LED trigger circuit design, suitable for fast switching at the determined radiation interval, was given in Fig. 2b. The optical power of the system was adjusted via controlling the current and calibrated with a power-meter and spectrometer.

2.2. Singlet oxygen detection system (SODS)

As shown in Fig. 1, the elements of the SODS were optic light collector, anti-reflective coated optical long pass filter, avalanche photodiode, high-frequency wide-bandwidth transimpedance amplifier, differential amplifier and an Arm-based microcontroller. These elements were introduced below.

2.3. Radiation collecting Lens system

The radiation collecting lens system consists of an optic collimation lens and 1250 nm long pass filter which were anti-reflective (AR) coated for 900 nm–1600 nm. The aim of this lens system was to focus the light on the middle point of the avalanche photodiode.

In Fig. 3, the collector lens distance diagram used to determine the optimum distance between the lens and focus point was given. In the figure, D is the height of the lens that gathers and collects the light from a source. The focal length f is the distance between the lens and focus point. Since the most of the resources were propagated from all angles, increasing D or decreasing f will allow the lens to capture more radiation. Thus, F is referred to as the *refraction index* and is the ratio of f and D. Finally, θ is the half angle of radiation cone.

The paraxial approach was commonly used as $F = \frac{f}{D}$, only for small angles (15°). The smaller the F-value, the higher the radial flux (c) collected by the lens. In Fig. 4, SODS system design was illustrated. Fig. 4 (a) shows probe handle design and phantom environment used for system evaluation, (b) gives the sections of the designed system.

2.3.1. APD transimpedance amplifier and differential amplifier circuit

Transimpedance amplifier (TIA) was designed to improve the performance of system along with various parameters such as gain, noise, speed, and bandwidth. Gain boost up can be done by using PMOS current source at the input stage. Capacitive coupling and cross-coupled current conveyor stage trim down input noise and increase the speed of transimpedance amplifier. The preferred op-amp was a broadband ultra-low noise TIA that supports APD applications.

An op-amp with wide bandwidth was the core of designed TIA block shown in Fig. 5. The CTRL (control pin) logical block controls an internal single-pole double-pulse (SPDT) switch to configure the gain of TIA. This pin also activates the internal feedback capacity required to correctly balance the amplifier. TIA circuit was designed to react between 50 KHz − 200 MHz bandwidth at the 4 GHz gain-bandwidth product (GBP).

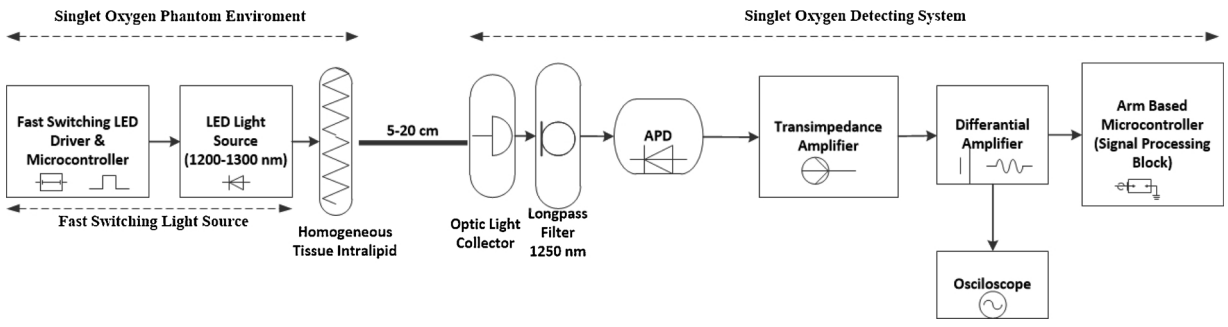

Fig. 1. Block diagram of the proposed setup.

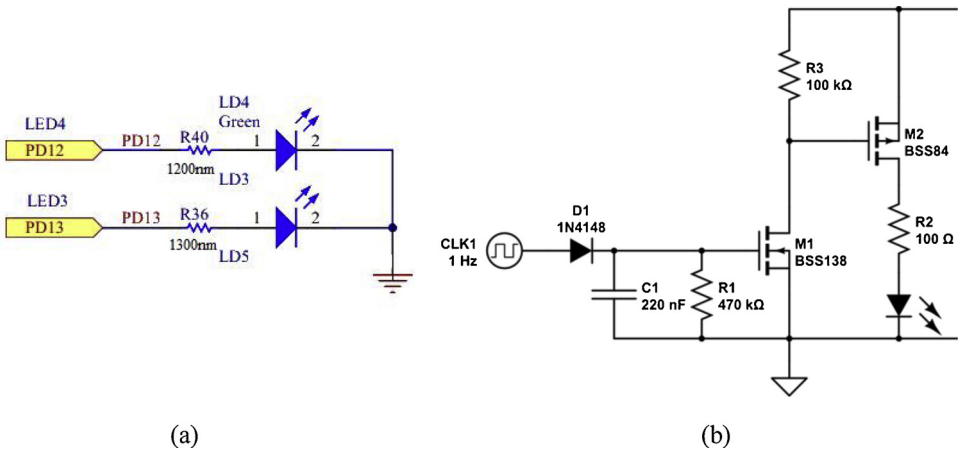

Fig. 2. a) LED-timer connection, b) Designed LED trigger circuit for fast switching.

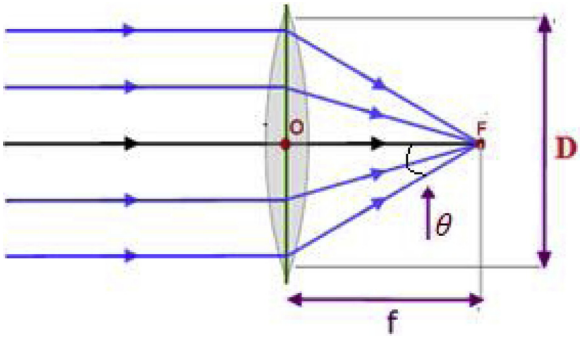

Fig. 3. The collector lens distance diagram.

As we know about operational amplifiers, all op-amps can be referred as a differential amplifier due to their input configurations. By connecting one voltage signal to the one input terminal and another voltage signal to the other input terminal, the resultant output voltage will be proportional to the difference between the two input voltage signals V1 and V2. In the designed amplifier circuits, system's frequency range was high and bandwidth was large for a typical application. Because of the sensitivity of system and broad response spectrum, capacitive effects of the resistors were considered for printed circuit board (PCB) design. In Fig. 6, the designed differential amplifier block was illustrated.

In the proposed differential amplifier circuit design, input and output pins of the op-amps have a fixing capability of approximately 2.5 V. Transformers provide both impedance matching and single-ended differential conversion. The circuit was designed with transformers having a 2:1 rotation ratio (4:1 impedance ratio) by matching the 200 O and 50 O impedance. A 2.2 nF load capacitor was placed between the resistors and the transformer. The 100 O resistor and the 2.2 nF capacitor create a snubber circuit that reduces the high-frequency peak and improves the stability.

2.3.2. Arm based signal processing block (Signal acquisition Module-SAM)

Signal processing circuit was designed to evaluate real-time singlet oxygen phosphoresce illumination. Two interfaces of the digital signal processing circuits, Analog Digital Converter (ADC) and Digital Analog Converter (DAC) were necessary to process analog signals in the digital environment and then convert them to the sensible form. In our system, the input of Arm-based signal processing block captures singlet oxygen phosphoresce illumination. In future works, the output of the processor is going to be used for PDT laser system to adjust the light dose and to calculate the pulse time.

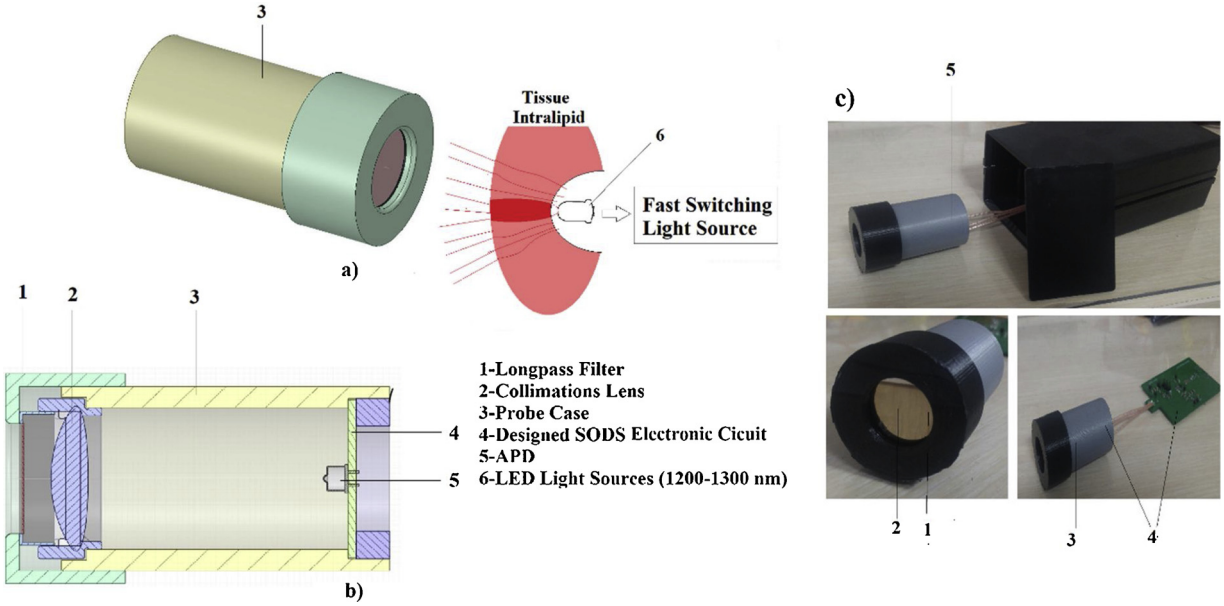

Fig. 4. SODS design illustration a) SODS probe and phantom environment, b) cross-sectional view of the designed system.

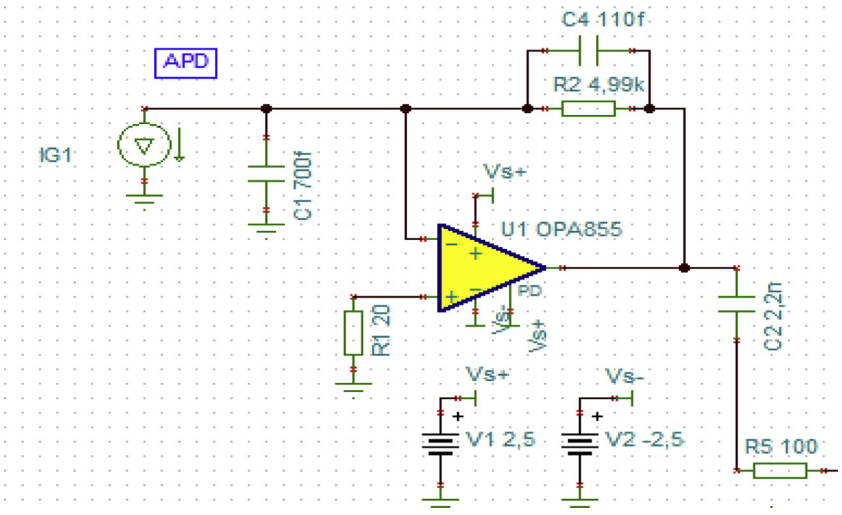

Fig. 5. The designed circuit that extends the bandwidth of TIA.

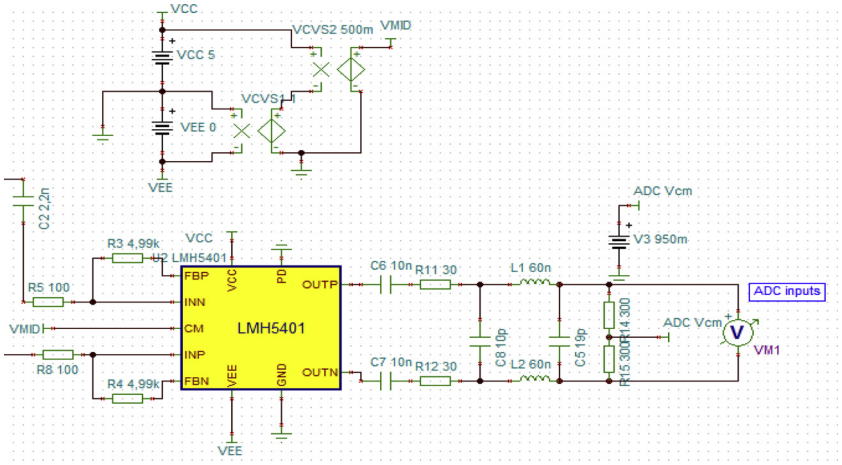

Fig. 6. Simplified differential amplifier circuit with Chebyshev filter for high-frequency signal detection.

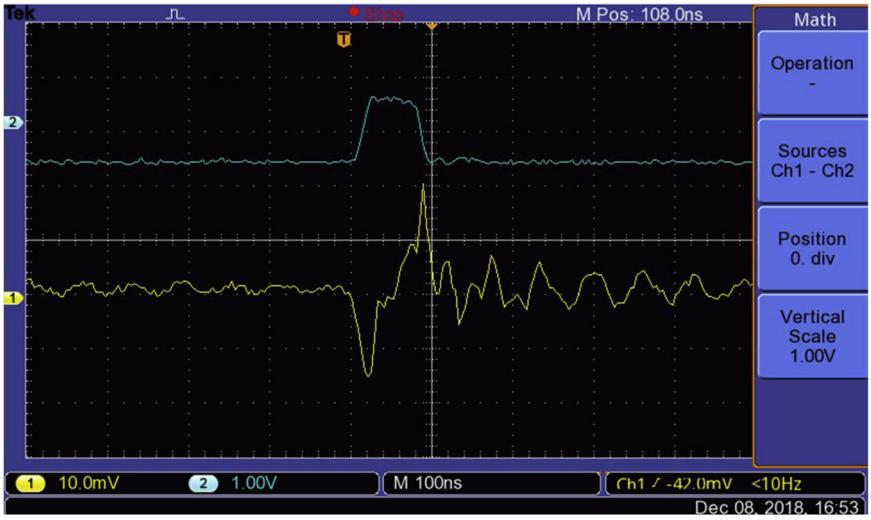

Fig. 7. The response of SODS system a 70 ns 1200 – 1300 nm pulse.

The designed circuits have a relatively small size and can be used for PDT application by integrating the fiber optic cable over the detector system.

3. Experimental results

In this section, singlet oxygen luminescence during PDT experiments were conducted in a phantom environment containing radiation between 1200 nm–1300 nm and tissue intra-lipid. In this experimental process, the target was to capture radiation at 1270 nm wavelength. Thus, the proposed system must be able to eliminate undesired wavelengths. Furthermore, the collimation lens provides more effective measurements, especially in femtowatt-level optic power measurement. The collector lens allows to detect optic power even at 2–5 fW level. Note that, if the optic lens was not used in SODS, it can measure 500 fW level optic power. So, collector lens combination makes the SODS sensitive to lover optic power levels.

The measurements were taken by means of the designed SODS, in accordance with the illumination level and life span of singlet oxygen. During the measurements, optic power and radiation duration were changed between 10 nW-1 mW and 20 ns-1 μs, respectively. After 2×10^5 amplification, it was observed that the system gave similar responses at different optical power level by virtue of applied signal processing and filtering methods.

At the first experiment, the response of the SODS to the pulse with 70 ns duration generated in the phantom environment was investigated. Differential response of the designed system was given in Fig. 7.

The aim of the experiment-2 was to discuss the performance of the designed system under noise. To improve the robustness of the system to noise, 1250 nm long pass optical filter was included to the SODS. By means of long pass optical filter, all undesired components were eliminated. After optic filter extension, response to the pulse with 70 ns duration and 1fW-1 nW optic power was shown in Fig. 8.

In Fig. 8, upper curves show the pulses and lower ones were the SODS response. As can be seen from the figure, noise components which have higher amplitudes than the desired signal was eliminated by using the optical filter. During the experiment, the distance between the LED source and the optic light collector was 5 cm.

In the following experiment (Experiment 3), the performance of the system to pulses having longer durations was investigated. The differential response of the system was taken at the edges of the pulses. The measured signals were given in Fig. 9.

By means of the performed experiments, the testing process of the SODS system was completed. According to the obtained results, it can be said that the system can measure short life, low-level luminescence around the 50 kHz-200 Mhz. Furthermore, by changing the distances between fast switching light source and SODS in 5 cm–20 cm interval, it was shown that the mobility of the designed system was high enough to use it in PDT by moving fiber optic cable with SODS system. Although a great number of experiments were conducted, only a few of them were given here not to extend the paper.

4. Validation of SODS measurements

SODS system can measure the different types of pulses with various optic powers and durations. The signals obtained at the output of the circuits were amplified by the designed system to make them processable. The purpose of this section was to validate the results obtained by the SODS system. For this purpose, mathematical analysis was performed. In this analysis, singlet oxygen luminescence intensity produced by the fast switching light source was calculated by mathematical equations. Then the intensity value was measured experimentally on the APD surface and compared with the mathematical result.

To predict the number of photons, generated by the light source and fall to the APD surface, intensity value must be calculated. During the mathematical calculations angle, area, distance, density and optical power were considered [35,36]. According to the literature, the optic power level used to obtain the number of photons expected to pass through the determined region is 0.05 pW for singlet oxygen in typical PDT applications [22–24,37].

The intensity of radiation emitted on a surface is known as normal radiation intensity (I_n) and can be expressed as follows:

$$I_n = \frac{\varepsilon G T^4}{\pi} \tag{1}$$

In Eq. (1), G is Stefan- Boltzmann constant (5,67x10^{-8} W/m^2k^4), T is absolute temperature and ε is the emissivity which is a function of emitted wavelength. However, in the proposed study, the radiation intensity is calculated related to the radiation produced by the LED. For this calculation, photon energy equation given in Eq. (2) is used.

$$E = h.c/\lambda \tag{2}$$

where c is light speed, λ is wavelength in meters and h is Planck constant. Since f = c/ λ, Equation (2) can be rewritten as

$$E = h.f \tag{3}$$

The parameter values for singlet oxygen are: λ = 1270 nm, f = 236,057.0535Ghz, and the photon energy is 0.9763 Ev. After calculating the energy of one photon, total energy on APD surface must be obtained. For this purpose, intensity-based reverse square law given in Eq. (4) is applied [37].

$$I = \frac{1}{2\mu_O c} E^2 \tag{4}$$

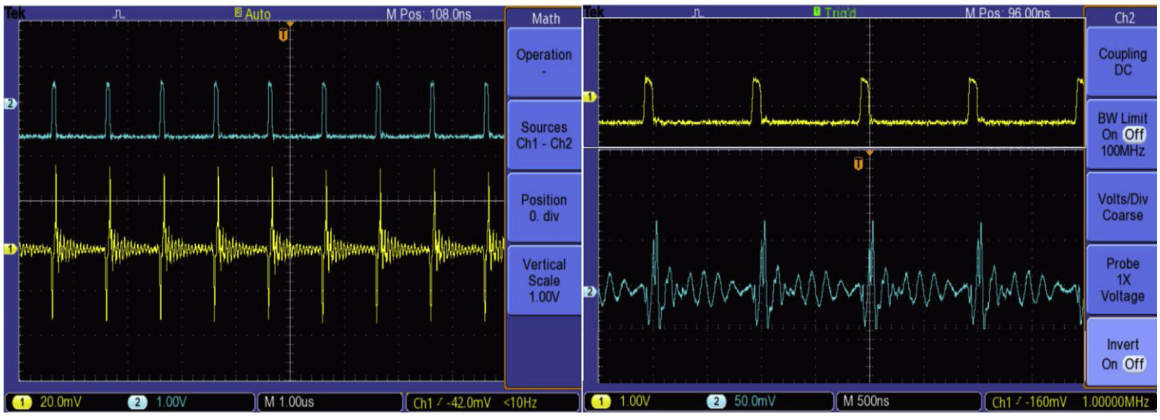

(a) (b)

Fig. 8. The response of the SODS system to 70 ns 1200 − 1300 nm pulses, a) under noise and b) after eliminating the noise.

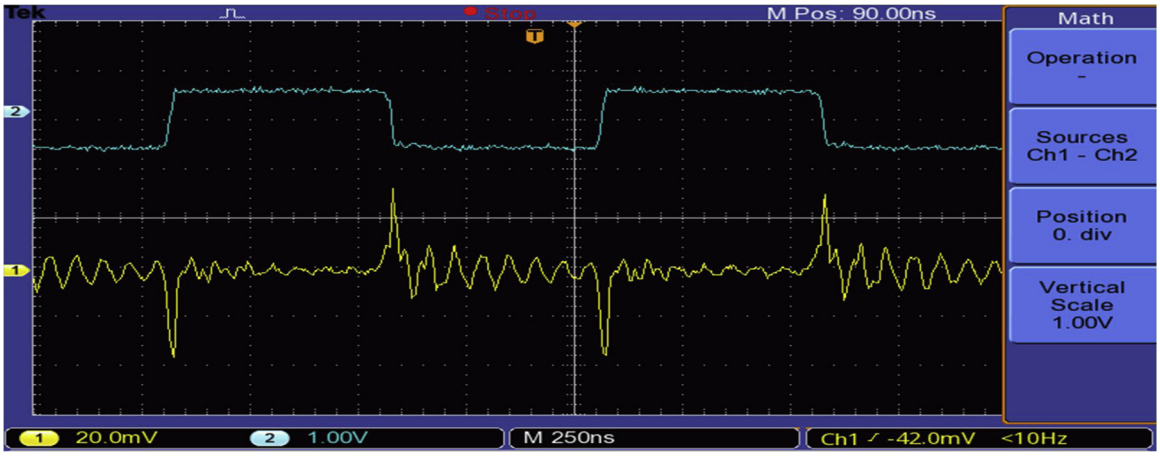

Fig. 9. SODS response to the pulses with longer durations (500 ns).

where μ_O is a constant and E is the photon energy calculated above. As a result of these calculations, the number of photons, that were predicted to be generated by the light source and failed to the sensitive area of the APD at the determined distance, was calculated over intensity value. The calculations were made considering the angle, area, distance, intensity, density and optical power.

In the light of mathematical analysis existing in the literature, it was obtained that when the distance between the light source and the APD surface was 5 cm, singlet oxygen luminescence intensity was 8500 (photon count) at femtowatt level. The photon number that fell to the APD surface was calculated from the electrical response of the system. When a photon hits the photodiode active zone, it can generate an electron-hole pair depending on the quantum efficiency of the device. Quantum yield depends on many factors, but if the energy of the photon was generally calculated by $E = h.\nu$, it was larger than the energy gap of the device, these photons were transformed into current by converting the photon motion to the electron particles on the surface where the recombination rate was high and will contribute to the measurements. The change of photodiode spectral properties with wavelength was explained by quantum efficiency. Semiconductor materials such as Silicon and InGaAs have different energy cavities; as a result, they exhibit different quantum yields at different wavelengths, resulting in spectral sensitivity profiles specific to the material type. Semiconductor photodiodes are ideal for low-level light measurements due to their high sensitivity and low noise characteristics. The SODS system voltage response to a number of photons calculated according to the ref [38–40]. The Johnson and Shot noise that affect the system was calculated via reference [41]. Noise components of the whole system were also measured.

The electrical response of the SODS system, which was used to calculate the singlet oxygen luminescence intensity, was achieved at first. Then, the noise components were eliminated. Finally, the intensity value was between 8000–12000 (photon count) and as an average of 9500 (photon count). In Fig. 10, measured average intensity values were demonstrated for 50.000 pulses. As can be seen from the figure, the system provides consistent results for singlet oxygen illumination.

Finally, the system is validated in the singlet oxygen phantom environment for different pulse durations. The optic power responses of SODS for different pulse durations are illustrated in Fig. 11. The measurements show that the proposed system can respond to the different illuminations with a stable response. The phantom environment can perfectly mimic artificial singlet oxygen illumination. Furthermore, the proposed phantom environment can behave like the different types of tissue phantom with a little adjustment and can be easily applied to the newly developed systems.

5. Discussion

In this study, the purpose was to design a system which has the ability to detect singlet oxygen illumination during PDT. For this purpose, SODS was developed and introduced. The performance of the system was evaluated with mathematical analysis and phantom environment measurements.

In the phantom environment, the experiments were performed in three groups in accordance with the illumination level and life span of the singlet oxygen. At the first experiment, the target was to show the

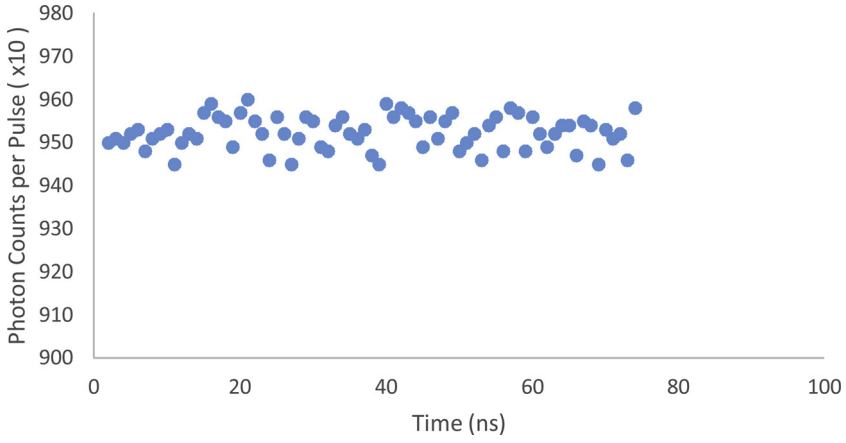

Fig. 10. The measured average intensity values for 70 ns pulses.

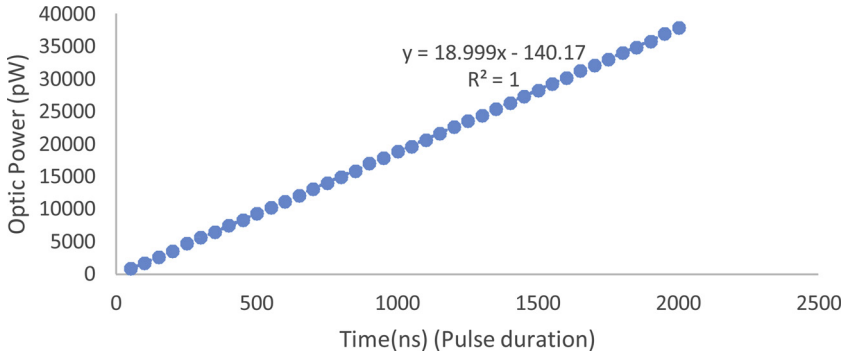

Fig. 11. The optic power response variation of SODS for different pulse durations.

response of SODS to 70 ns pulses. Because of the life span of singlet oxygen changes between 10 ns and 1–2 u s, similar to the existing studies in the literature, 70 ns pulses were preferred for performance evaluation. According to the results of the experiment-1, the designed system can detect these pulses reliably (Fig. 7). Experiment-2 was conducted to discuss the response of SODS under noise. The existence of 1250 nm long-pass filter makes the system robust to the optical noises. So, the pulse response of the designed system to 70 ns pulses under noise was as desired (Fig. 8). In the experiment-3, the performance of the system is tested for pulses with longer durations. For this investigation, 500 ns pulses were applied to the system and then the differential response of the system was measured (Fig. 9). Furthermore, the measured average intensity values were demonstrated for 50.000 pulses to manifest that the proposed system provides consistent results for singlet oxygen illumination (Fig. 10). Finally,

the system is validated in the singlet oxygen phantom environment for different pulse durations. For this purpose, pulse durations are changed from 50 ns to 2000 ns and the corresponding optic power values are measured. The measurements show that the proposed system can respond to the different illuminations with a stable response. The results of all conducted experiments exhibit that the SODS was able to detect singlet oxygen illumination. So, SODS can be combined with the PDT laser device for successful treatment.

After pulse response experiments, singlet oxygen luminescence intensity obtained by the SODS was validated. Therefore, a comparison between mathematical calculations and experimental measurements was made based on intensity value. The obtained results showed that the experimental and mathematically calculated intensity values were compatible.

The presented study was compared with the most similar studies in the literature to prove its contributions, at first. N.R. Gemmell et al. 2013 [28], the authors aim to monitor singlet oxygen luminescence. They employ a low noise superconducting nanowire single-photon (SNSPD) to record singlet oxygen luminescence at 1270 nm wavelength from a model photosensitizer (Rose Bengal) in solution. In their system design, they combined armored fiber to SNSPD. Due to fiber-optic cables inherent properties, optic power can be decreased during the transmission. In the SODS design, instead of using fiber optic cable, collimation is directly focused on the APD surface. So, optic power loss was avoided. Furthermore, SNSPD was a general purpose device used for photon detection. However, the proposed SODS system was specially designed for the low-optic power and high-frequency singlet oxygen luminescence detection. N.R. Gemmell et al. 2017 [29], the authors improved their SNSPD system by using single-photon avalanche diode detector (SPAD). The overall system performance in term of count rate and signal-to-noise ratio was improved by 50-fold-over fiber-coupled SNSPD system. However, optic power loss raised from fiber optic cable usage still exists. Although the goal of [29] was fairly similar to the proposed study and it was a promising study for PDT researches, the cost of the system was higher (~21.000 €). One of the contributions of the SODS was its lower cost (~1200 €) that made it easy procurable for clinical researches. In this study [30], Boso and his friends designed a practical setup based on a negative-feedback avalanche diode (NFAD) detector. They used NFAD to detect singlet oxygen. Its frequency interval was between 1 Hz and 20 MHz which made it impossible to use with new type PDT laser systems introduced in H.S. lim et. al. 2012 [4]. In the presented design, signals with 50 kHz – 200 MHz can be detected. This frequency interval is compatible with the new type of PDT laser systems. In addition, several types of filters are included to overcome the noise affects, whereas, in our system, two filters were applied to the signals. The study given with G. Boso et al. 2016 [30], chemical-based optical phantom system, which had difficulties in the preparation stage, was constructed to evaluate the performance of the whole system. In the SODS, an electronic-based phantom system which was user-friendly, had adjustable illumination level and did not require a pre-preparation phase. As far as we know, this study is the first study which constructs a phantom environment with femtowatt level optical power.

At the end of the discussion section, Table 1 was prepared to better discuss the situation of the proposed study in the literature. This reference table is constructed to point out the important aspects of the valuable studies and to compare them with the presented study. According to this literature review, the following assessments can be made:

In the singlet oxygen illumination range, NIR photomultiplier tubes and newly developed InGaAs cameras have been mainly used as a single-photon detector. InGaAs cameras were used with an external electronic circuit and photon trigger but even though having a large active area (> 10 mm x 10 mm) and high efficiency (> 30–50%) the speed of the cameras could not be operated in the range of singlet oxygen luminescence illumination life time [42]. Then, the PMTs were widely used in the singlet oxygen luminescence detection field [43–46]. Their main advantage was having a large active area (> 10 mm) that was essential to collect photons from large diffusing samples. Unfortunately, they have many disadvantages like very low quantum efficiency (< 1%), moderate noise (> 10,000 cps), delicate photocathode (it can be corrupted by ambient light) and the difficulty to gate the detector to suppress stray light during measurement. The newly developed SPADs started to be used in the singlet oxygen detection studies due to their higher detection efficiency, lower noise sensitivity, compact form factor, stability, ease-of-use and the possibility to be gated [47–49]. However, SPADs' gated-mode operation could not cooperate with the singlet oxygen luminescence in NIR wavelength range due to their wider illumination ranges (> 40 ns *in vivo*, > 3 µs) [50,51]. The newly developed superconducting nanowire single-photon detectors (SNSPDS) presented an alternative measurement system for PDT applications but the clinical adaptation seems like a quite limited because of the size, cost and difficulty in usage [28].

In reference [52] direct SOLD measurements were compared with the singlet oxygen explicit dosimetry (SOED) calculations for phantoms using Photofrin and SPAD. The oxygen and PS concentration

Table 1
The comparison of the proposed study with the available studies.

Reference Number	System	Bandwidth	Efficiency	Active Area	Fiber Optic Cable	Anti-reflective Coated Lens and Collector for NIR Region	Specially Designed for PDT	Clinical Potential	Cost
[42]	InGaAs Camera	–	> 30-50%	> 10 × 10 mm	No	No	No	Medium	> 10.000 £
[43,44,45,46]	PMT	DC-GHz	< 1%	> 10 mm	No	No	No	Low	> 50.000 £
[47,48,49]	SPAD	DC-100KHz	> 50%	20 µm – 500 µm	Yes	No	No	Medium-higher	> 20.000 £
[28]	SNSPDS	> 10 GHz	> 50%	10 µm – 300 µm	Yes	No	No	Low	> 20.000 £
[30,50]	NFAD	DC- GHz	> 10%	10 µm – 500 µm	Yes	No	No	Relatively higher	> 5.000 £
The proposed study	SODS	100kHz – 200 MHz	> 50%	4 mm	No	Yes	Yes	Relatively higher	> 1.000 £

measurements were compared with SOED predictions to validate the SOED model. The results showed that there was a direct correlation between SOLD and SOED. However, the system could be further improved by using a specially designed singlet oxygen measurement system. So far, different systems were designed for PDT treatment modalities. The system limitations could be found with the electronic-based phantom environment without using complex laboratory equipment. The SOED based models could be implemented in a phantom environment for mimicking the singlet oxygen luminescence for further exploitation and could be compared with SOLD based measurements without using a computer and laboratory equipment. The phantom environment prevents the impairment of laboratory equipment and provides stable light level measurements.

The last row of Table 1 gives the important points of the proposed study. The main advantage of the system is its lower cost which makes is easily accessible for PDT experiments. Furthermore, its efficiency, antireflective coated lens and collector, special design, and clinical potential makes it attractive among its competitors. In the light of the above discussions, it can be concluded that the proposed SODS system will be a good candidate for clinical PDT applications after further experimental analysis.

Acknowledgment

This study is supported by TUBITAK and Sakarya University with project numbers 118E235 and 2017-50-02-027, respectively.

References

[1] B.C. Wilson, M.S. Patterson, The physics of photodynamic therapy, Physics in Medicine & Biology vol. 31, (no. 4) (1985).
[2] B.C. Wilson, M.S. Patterson, The physics, biophysics and technology of photodynamic therapy, Phys. Med. Biol. 53 (2008) R61–R109.
[3] F.W. Hetzel, S.M. Brahmavar, Q. Chen, S.L. Jacques, M.S. Patterson, B.C. Wilson, T.C. Zhu, The american association of physicists in medicine, photodynamic therapy dosimetry, AAPM report No. 88, Medical Physics Publishing for the American Association of Physicists in Medicine (2005).
[4] H.S. Lim, Reduction of thermal damage in photodynamic therapy by Laser irradiation techniques, J. Biomed. Opt. 17 (12) (2012) 1–9 128001.
[5] C.P. Neckel, Comparative study on CW-mode versus pulsed mode in A1GaAs-diode Lasers, Proc. SPIE. Int. Soc. Opt. Eng. 4249 (2001) 44–49.
[6] M. Panjehpour, B.F. Overholt, R.E. Sneed, R.C. DeNovo, M.G. Petersen, Comparison between pulsed and continuous wave Lasers for photodynamic therapy, Proc. SPIE. Int. Soc. Opt. Eng. 1881 (1993) 319–324.
[7] K. Matthewson, P. Coleridge-Smith, T.C. Northfield, S.G. Bown, Comparison of continuous-wave and pulsed excitation for interstitial Neodymium-YAG Laser induced hyperthermia, Lasers Med. Sci. 1 (1986) 197–201.
[8] J.W. Feather, I. Driver, P.R. King, C. Lowdell, B. Dixon, Light delivery to tumor tissue through implanted optical fibers during photodynamic therapy, Lasers Med. Sci. 5 (1990) 345–350.
[9] W.M. Star, Light delivery and light dosimetry for photodynamic therapy, Lasers Med. Sci. 5 (1990) 107–113.
[10] L.H. Murrer, J.P. Marijnissen, W.M. Star, Light distribution by linear diffusing sources for photodynamic therapy, Phys. Med. Biol. 41 (1996) 951–961.
[11] P.R. Ogilby, Singlet oxygen: There is indeed something new under the sun, Chem. Soc. Rev. vol. 39, (no. 8) (2010) 3181–3209.
[12] M.C. DeRosa, R.J. Crutchley, Photosensitized singlet oxygen and its applications, Coordination Chem. Rev. vol. 233–234, (2002) 351–371.
[13] C. Schweitzer, R. Schmidt, Physical mechanisms of generation and deactivation of singlet oxygen, Chem. Rev. vol. 103, (no. 5) (2003) 1685–1757.
[14] T.S. Mang, Lasers and light sources for PDT: past, present and future, Photodiagnosis Photodyn, Ther 1 (2004) 43–48.
[15] T.J. Dougherty, et al., Photodynamic therapy, J. Natl. Cancer Inst. vol. 90, (no. 12) (1998) 889–905 Jun..
[16] G. Yu, et al., Noninvasive monitoring of murine tumor blood flow during and after photodynamic therapy provides early assessment of therapeutic efficacy, Clin. Cancer Res. vol. 11, (no. 9) (2005) 3543–3552.
[17] M.T. Jarvi, M.J. Niedre, M.S. Patterson, B.C. Wilson, Singlet oxygen luminescence dosimetry (SOLD) for photodynamic therapy: Current status, challenges and future prospects, Photochem. Photobiol. vol. 82, (no. 5) (2006) 1198–1210.
[18] B.C. Wilson, M.S. Patterson, L. Lilge, Implicit and explicit dosimetry in photodynamic therapy: A New paradigm, Lasers Med. Sci. vol. 12, (no. 3) (1997) 182–199.
[19] R.A. Weersink, et al., Techniques for delivery and monitoring of TOOKAD (WST09)-mediated photodynamic therapy of the prostate: Clinical experience and practicalities, J. Photochem. Photobiol. vol. 79, (no. 3) (2005) 211–222.
[20] M.S. Thompson, et al., Clinical system for interstitial photodynamic therapy with

combined on-line dosimetry measurements, Appl. Opt. vol. 44, (no. 19) (2005) 4023–4031 Jul..
[21] T.C. Zhu, J.C. Finlay, S.M. Hahn, Determination of the distribution of light, optical properties, drug concentration, and tissue oxygenation *in vivo* in human prostate during motexafin lutetium-mediated photodynamic therapy, J. Photochem. Photobiol. vol. 79, (no. 3) (2005) 231–241 Jun..
[22] H. Zeng, M. Korbelik, D.I. McLean, C. MacAulay, H. Lui, Monitoring photoproduct formation and photo bleaching by fluorescence spectroscopy has the potential to improve PDT dosimetry with a verteporfinlike photosensitizer, Photochem. Photobiol. vol. 75, (no. 4) (2002) 398–405. Apr..
[23] I. Georgakoudi, M.G. Nichols, T.H. Foster, The mechanism of Photofrin photo bleaching and its consequences for photodynamic dosimetry, Photochem. Photobiol. vol. 65, (no. 1) (1997) 135–144 Jan..
[24] J.S. Dysart, M.S. Patterson, Photo bleaching kinetics, photoproduct formation, and dose estimation during ALA induced PpIX PDT of MLL cells under well oxygenated and hypoxic conditions, Photochem. Photobiol. Sci. vol. 5, (no. 1) (2006) 73–81 Jan..
[25] A. Molckovsky, B.C. Wilson, Monitoring of cell and tissue responses to photodynamic therapy by electrical impedance spectroscopy, Phys. Med. Biol. vol. 46, (no. 4) (2001) 983–1002. April..
[26] D. Lapointe, et al., High-resolution PET imaging for *in-vivo* monitoring of tumor response after photodynamic therapy in mice, J. Nucl. Med. vol. 40, (no. 5) (1999) 876–882 May.
[27] M. Niedre, M.S. Patterson, B.C. Wilson, Direct near-infrared luminescence detection of singlet oxygen generated by photodynamic therapy in cells in vitro and tissues *in vivo*, Photochem. Photobiol. vol. 75, (no. 4) (2002) 382–391. Apr.
[28] Nathan R. Gemmell, Aongus McCarthy, Baochang Liu, Michael G. Tanner, Sander D. Dorenbos, Valery Zwiller, Michael S. Patterson, Gerald S. Buller, Brian C. Wilson, Robert H. Hadfield, Singlet oxygen luminescence detection with a fiber coupled superconducting nanowire single-photon detector, Opt. Express vol. 21, (no. 4) (2013) 5005–5013 Feb..
[29] N.R. Gemmell, A. McCarthy, M.M. Kim, I. Veilleux, T.C. Zhu, G.S. Buller, B.C. Wilson, R.H. Hadfield, A compact fiber-optic probe-based singlet oxygen luminescence detection system, J. Biophoton. vol. 10, (no. 2) (2017) 320–326 Feb..
[30] G. Boso, et al., Time-resolved singlet-oxygen luminescence detection with an efficient and practical semiconductor single-photon detector, Biomed. Opt. Express vol. 7, (no. 1) (2016) 211–224 Dec..
[31] Robert H. Hadfield, Single-photon detectors for optical quantum information applications, Nature Photon. vol. 3, (2013) 696–705 Dec..
[32] S. Lee, K. Galbally-Kinney, M.F. Hinds, J.A. O'Hara, B.W. Pogue, A. Liang, T. Hasan, S.J. Davis, A singlet oxygen monitor as an *in vivo* photodynamic therapy dosimeter, Proceedings of SPIE - The International Society for Optical Engineering, 2009.
[33] Sooyeon Kim, Takashi Tachikawa, Mamoru Fujitsuka, Tetsuro Majima, Far-Red Fluorescence Probe for Monitoring Singlet Oxygen During Photodynamic Therapy 136 American Chemical Society, 2014, pp. 11707–11715.
[34] Marek Scholz, Roman Dědic, Jan Valenta, Thomas Breitenbach, Jan Hála, Real-time luminescence micro spectroscopy monitoring of singlet oxygen in individual cells, Photochem. Photobiol. Sci. 13 (2014) 1203.
[35] S.M. Popoff, A. Goetschy, S.F. Liew, A.D. Stone, H. Cao, Coherent control of total transmission of light through disordered media, Phys. Rev. Lett. 112 (2014) 133903.
[36] W. Choi, M. Kim, D. Kim, C. Yoon, C. Fang-Yen, Q.-H. Park, W. Choi, Preferential coupling of an incident wave to reflection Eigen channels of disordered media, Sci. Rep. 5 (2015) 11393.
[37] Hsiang-Yu Lo, Po-Ching Su, Yu-Wei Cheng, Pin-I. Wu, Yong-Fan Chen, Femtowatt-light-level phase measurement of slow light pulses via beat-note interferometer, Opt. Express vol. 18, (No. 17) (2010) 18498.
[38] Jiao Xu, Xiaoshuang Chen, Wenjuan Wang, Wei Lu, Extracting dark current components and characteristics parameters for InGaAs/InP avalanche photodiodes, Infrared Phys. Technol. vol. 76, (2016) 468–473 May.
[39] Yufa Zhang, Xianan Dou, Feng Li, Xiaoquan Sun, The response characteristics of avalanche photodiodes to ultrashort pulsed laser, Infrared Phys. Technol. vol. 73, (2015) 226–231 November.
[40] Y. Uliel, D. Cohen-Elias, N. Sicron, I. Grimberg, N. Snapi, Y. Paltiel, M. Katz, In GaAs/GaAsSb Type-II super lattice based photodiodes for short wave infrared detection, Infrared Phys. Technol. vol. 84, (2017) 63–71. August.
[41] Guipeng Liu, Xin Wang, Jingze Zhao, Wenjie Chen, Yonghui Tian, Jianhong Yang, Modeling a novel InP/InGaAs avalanche photodiode structure: Reducing the excess noise factor, Communications 435 (2019) 374–377.
[42] Weitao Li, Dong Huang, Yan Zhang, Yangyang Liu, Yueqing Gu, Zhiyu Qian, Real-Time Monitoring of Singlet Oxygen and Oxygen Partial Pressure During the Deep Photodynamic Therapy In Vitro, Ann. Biomed. Eng. vol. 44, (No. 9) (2016) 2737–2745.
[43] A. Jimenez-Banzo, X. Ragas, P. Kapusta, et al., Time-resolved methods in biophysics. 7. Photon counting vs. analog time-resolved singlet oxygen phosphorescence detection, Photochem. Photobiol. Sci. 7 (9) (2008) 1003.
[44] J. Schlothauer, S. Hackbarth, B. Roder, A new benchmark for time-resolved detection of singlet oxygen luminescence — Revealing the evolution of lifetime in living cells with low dose illumination, Laser Phys. Lett. 6 (3) (2009) 216.
[45] B. Li, H. Lin, D. Chen, et al., Detection system for singlet oxygen luminescence in photodynamic therapy, Chin. Opt. Lett. 8 (1) (2010) 86.
[46] W. Baumler, J. Regensburger, A. Knak, et al., UVA and endogenous photosensitizers—The detection of singlet oxygen by its luminescence, Photochem. Photobiol. Sci. 11 (1) (2012) 107.
[47] I. Coto Hernández, M. Buttafava, G. Boso, A. Diaspro, A. Tosi, G. Vicidomini, Gated STED microscopy with time-gated single-photon avalanche diode, Biomed. Opt. Express 6 (6) (2015) 2258–2267.
[48] M. Mazurenka, L. Di Sieno, G. Boso, D. Contini, A. Pifferi, A.D. Mora, A. Tosi, H. Wabnitz, R. Macdonald, Non-contact in vivo diffuse optical imaging using a time-gated scanning system, Biomed. Opt. Express 4 (10) (2013) 2257–2268.
[49] E. Alerstam, T. Svensson, S. Andersson-Engels, L. Spinelli, D. Contini, A. Dalla Mora, A. Tosi, F. Zappa, A. Pifferi, Single-fiber diffuse optical time-of-flight spectroscopy, Opt. Lett. 37 (14) (2012) 2877–2879.
[50] T. Lunghi, C. Barreiro, O. Guinnard, R. Houlmann, X. Jiang, M.A. Itzler, H. Zbinden, Free-running singlephoton detection based on a negative feedback InGaAs APD, J. Mod. Opt. 59 (17) (2012) 1481–1488.
[51] I. Bargigia, A. Tosi, A. Bahgat Shehata, A. Della Frera, A. Farina, A. Bassi, P. Taroni, A. Dalla Mora, F. Zappa, R. Cubeddu, A. Pifferi, Time-resolved diffuse optical spectroscopy up to 1700 nm by means of a time gated InGaAs/InP single-photon avalanche diode, Appl. Spectrosc. 66 (8) (2012) 944–950.
[52] M.M. Kim, R. Penjweini, N.R. Gemmell, I. Veilleux, A. McCarthy, G.S. Buller, R.H. Hadfield, B.C. Wilson, T.C. Zhu, A comparison of singlet oxygen explicit dosimetry (SOED) and singlet oxygen luminescence dosimetry (SOLD) for photofrin-mediated photodynamic therapy, Cancers (Basel) 6 (12) (2016) 109 8.